Cross-consistency of system and characteristic-field models in a coupled liquid-rocket simulation (Merlin 1D–class case study)

Daniel Sim

Independent researcher; LorenLib development, Open Space Launch Ltd; Meco Rocket Simulator, Loren Aerospace Ltd

***Abstract*—Coupled liquid-rocket system models and multidimensional nozzle solvers are usually developed separately; when they are made to share a chamber state, the mass-flow consistency between them is easy to leave unmeasured. We describe a transient LOX/RP-1 open-cycle gas-generator engine architecture — capacitance–inertance liquid feed networks, a compressible gas-flow network, shaft dynamics, multi-layer regenerative wall response, offline equilibrium thermochemistry tables, and orifice injector hydraulics — coupled at analysis stop to an axisymmetric method-of-characteristics (MOC) nozzle field evaluated at the shared chamber stagnation state. A headless extraction harness regenerates all tabulated results from frozen inputs and grades two mass residuals: conservation through the marched nozzle field, and agreement between field and system mass flow. The architecture is demonstrated on a Merlin 1D–class case assembled from public data. On the frozen case, field mass conservation closes to +0.92%, the field–system mass-flow residual is -1.78%, sea-level field thrust is ~831 kN, and engine specific impulse on total propellant flow (~305 kg/s) is ~277.7 s, consistent with the public Merlin-class bands that guided case authoring. The result is a documented, reproducible open-cycle composition in which system–field consistency is measured rather than assumed; the case study is a representative reconstruction, and all artefacts are archived on Zenodo.**

***Index Terms*—liquid rocket propulsion; gas-generator cycle; system modelling; method of characteristics; verification; Meco Rocket Simulator**

Preprint. v0.6.0. 2026-08-10. **Input deck:** `64f364d6a43c50d7 a2f7f77bddef235f`. **Software archive:** `00312a51`.
DOI: `10.5281/zenodo.21878536` (concept `10.5281/zenodo.21864769`). **Software:** LorenLib (system model + geometry/MOC). **Venue:** engrXiv (primary preprint) + Zenodo (PDF + data/code archive DOI). *Note:* Primary contribution: coupled open-cycle GG architecture with freeze provenance and extractable consistency metrics. Merlin numbers are case outcomes on a frozen fixture (§3.2), not flight validation. Interactive authoring used Meco Rocket Simulator (commercial; mecorocketsimulator.com); tables use headless LorenLib extracts.

I. Introduction

Coupled liquid-rocket **system** codes and multidimensional **nozzle** solvers are often developed separately. A single, documented open-cycle GG stack that integrates feeds, gas network, shafts, walls, and thermochemistry through spin-up and evaluates an independent MOC field at shared chamber state—with frozen, citable extracts—is less common than either algebraic cycle sheets or standalone MOC packages.

This paper's primary object is that **architecture** (composition of the transient system + field path + extract workflow). Mass residuals ($r_{\text{conservation}}$, r_{network}) and claim discipline (unreconciled F_{field} as headline; density-linear F' co-reported with k so the field–network mass basis is explicit; engine Isp on total propellant) complete that package. We deliberately leave the field–network mass delta open rather than closing it with a throat discharge coefficient: a measured residual is what makes the system–field interface checkable (§4.1).

Public Merlin 1D data [1]–[3] support **class-band** case definition but not a flight digital twin. We use a Merlin 1D–class open-cycle GG **case study** with an explicit split between the **baseline system model** (which elements exist) and **author-selected parameters** for the frozen fixture (§3.2).

Contributions.

1. A **coupled transient open-cycle GG system architecture** (liquid feed, gas network, shafts, walls, thermochemistry tables, injectors) with post-stop axisymmetric MOC field and a reproducible extract workflow archived on **Zenodo**.
2. **Extractable consistency metrics** ($r_{\text{conservation}}$, r_{network}, 1-D choke anchor) so system↔field mass bookkeeping is visible in the paper tables.
3. A Merlin-class **case study** with frozen inputs and a clear split of baseline elements vs selected parameters (§3)—outcomes on that case, not flight validation.
4. Claim discipline: unreconciled F_{field} is the headline; density-linear F' is co-reported with k as a mass-basis diagnostic; engine Isp uses total propellant (MCC+GG).

Outside the contribution list. Classical mass-conserving curved startline (Sauer / Kliegel–Levine lineage) for finite throat curvature; §4.1 records a constant-z seed only as a **negative control** that the residuals respond. No new transonic theory.

Non-claims (binding). No flight telemetry match; no ~200 atm pump-discharge figure from secondary online reconstructions as Public hardware truth; no quasi-1D nozzle F; no dual-path divergence science; no F' as independent 845 kN validation; no new Sauer/KL theory; no claim that continuous fixture parameters are uniquely determined by public data (§3.2).

II. Methods

A. System architecture

The dynamic model is fixed-step explicit RK4 integration of indexed ODEs for liquid branches, gas-network elements, turbomachinery shafts, and multi-layer solid walls (LorenLib system model), advanced at a fixed step $\Delta t = 2 \times 10^{-5}$ s on the frozen case (10^5 steps over the 2.0 s horizon). On this case the 2.0 s horizon integrates in ≈1.9 s wall-clock — faster than real time — and the complete MOC thrust extract (transient + field march + thrust tables) finishes in ≈8 s, on a single Apple M2 Pro core (release build).

Liquid feed (capacitance–inertance). Liquid internal nodes accumulate mass via hydraulic capacitance $C = \kappa\rho V$ [kg/Pa]; branches evolve $\dot{m}$ as inertance ODEs driven by end-to-end Δp. That lumped capacitance–inertance class is the standard EcosimPro / ESPSS-style LRE system-modelling pattern. We cite the EcosimPro Users Meeting liquid-rocket demonstration [10] for system-level heritage of this formulation, and MIT 16.512 *Rocket Propulsion* notes [11] for the cryogen compressibility / κ scale used for LOX-class fluids. Capacitance floors and vapor-pressure limits are numerical stabilisations specific to this implementation.

Gas network (flow-network residual + LMA). The gas side is a **network-primary** steady residual on junction static pressures and element mass flows, closed by a damped-Newton / Levenberg–Marquardt (LMA-style) outer loop [13] (problem-specific implementation; the classical LMA name marks the damping heritage only). The 1-D compressible **flow-network** architecture — mass coupling at nodes, element conductances, nodal solution — is informed by Sultanian, *Gas Turbines: Internal Flow Systems Modeling* (Cambridge University Press, 2018) [12]. Classical gas-network simulation literature (Osiadacz-class pipeline networks) [14] is complementary context. Detailed residual assembly and solver controls are documented in the companion design specification (Zenodo package).

Startup uses chained control-parameter schedules (fuel-lead ordering: the RP-1 valve ramps trigger before the LOX ramps on a shared startup sequence signal). The integration horizon for quasi-steady tables is $t = 2.0\,\text{s}$ — an **integration choice** rather than a representation of the flight spin-up timeline.

Terminology — "open". **Open-cycle** means the gas-generator thermodynamic cycle: GG exhaust is dumped separately from the MCC (not "open-source software"). Where software availability is meant, this paper points to the **Zenodo** archival snapshot (PDF, frozen case definition, extract tables, executable + data snapshot).

1) Implementation tooling: The dynamical model and MOC field are implemented in **LorenLib**, a methods library developed by Open Space Launch, which is working toward an open-source release of the library, planned under GPLv2 with the Universal FOSS Exception (licence and availability terms in the companion design specification). The Merlin-class case in this paper was **authored and interactively inspected** in **Meco Rocket Simulator** (Loren Aerospace): a commercial desktop application that embeds LorenLib for engine layout editing, parameter setting, startup scheduling, and on-screen visualisations of network topology, fields, and time histories. Meco is the interactive front-end used to *build and explore* the frozen case (engine layout and parameter authoring that produce the frozen JSON deck); all governing equations, ODE integration, MOC marching, and headless extraction are implemented in LorenLib.

Reproducing the quantitative tables in this manuscript does not require Meco: extract tables and the headless LorenLib path ship with the **Zenodo** archive (§3.1). Availability of both tools is stated in the *Software and data availability* section.

Quantitative tables (settle windows, MOC thrust, conservation diagnostics) are regenerated with a **headless LorenLib extract** on the frozen case, not transcribed from product UI cards (F' is co-reported with F_{field} in §4.1 as a density-linear diagnostic). If a figure is produced in Meco for illustration only, the caption states that quantitative values come from the tabulated extracts. Full attribution, licence, and reproduction recipe: companion design specification in the **Zenodo** package.

B. Thermochemistry, combustion model, and injector hydraulics

Equilibrium thermochemistry (offline tables). Hot-gas LOX/RP-1 properties come from offline equilibrium tables: generators (CEA-class / rocketcea-style equilibration) precompute lookup tables on a $(p_c,\ o/f)$ grid, and at run time the model interpolates combustion temperature and thermo-transport state (T_0, γ, r_s, c_p, μ, $\ldots$) from those tables given local oxidizer and fuel mass rates and chamber pressure. No chemical kinetics are integrated at runtime. Derived quantities such as c^* and isentropic relations use standard compressible-flow relations as implemented in LorenLib.

Combustion assumptions at gas-generator and chamber heads. MCC and GG heads are modelled as gas sources that **emit** equilibrated combustion products:

- complete mixing of oxidizer and fuel feeds at the head;
- **instantaneous thermodynamic equilibrium** at the local chamber pressure and mixture ratio $o/f = \dot{m}_o/\dot{m}_f$ (table lookup, not finite-rate kinetics);
- liquid and gas networks couple **thermodynamically** (emitted gas state from tables), not by enforcing species-level mass continuity between liquid injector $\dot{m}$ and gas $\dot{m}$ (measured discrepancy on related cases is expected);
- no explicit combustion-efficiency η_{c^*} scalar is applied as a free paper knob on this freeze—departure from ideal c^* is absorbed only through table physics, geometry, and the emergent network solve. This matters for reading §4: equilibrium-table combustion is an upper bound on c^* ($\eta_{c^*} = 1$ by construction, where real LOX/RP-1 chambers deliver roughly 0.92–0.995 of ideal c^* [21]), so T_0 and c^*-scale quantities carry a known-direction bias that is disclosed rather than tuned away — and near-band agreement in §4.2 is reached without an efficiency fudge factor.

The start-up traces in §4.5 accordingly demonstrate feed–network–shaft dynamics; ignition and flame-establishment transients are outside the model.

Injector–chamber hydraulic coupling. LOX and RP-1 injectors on the freeze are **discharge-law orifices**, not plain friction pipes. The quasi-steady incompressible orifice law is of the form

$$\dot{m}^* = C_d\, A\sqrt{2\rho\,\Delta p_{\text{eff}}},$$

implemented as a branch $\dot{m}$ ODE driven toward that target. Author-selected C_d, geometric area (circle or annulus), and multiplicity n set injector Δp–$\dot{m}$ share (§3.2). The selected C_d (0.7 radial / 0.8 annular) are pintle design-space norms sitting within the measured sharp-edge (0.61) to short-tube (0.82) orifice classes compiled in NASA SP-8089 [37], whose reported ~15% as-drilled fabrication scatter exceeds that spread. This bridges liquid feed headers to gas-generator / chamber heads without modelling droplet atomization, vaporization delay, or 3D spray pattern.

Liquid transport / coolant. Liquid ρ, μ, κ (for capacitance) are table-driven for LOX and RP-1, evaluated at fixed feed states: RP-1 subchilled to 266.15 K (-7 řC, Falcon 9 Full Thrust practice); LOX 2 K below saturation at the 4 bar table pressure — near-boiling feed, not densified-LOX practice (a construction that shows up as the thin LOX NPSH margin in §4.2). Coolant bulk temperature is read from the liquid feed state, with no bulk-enthalpy ODE (one-way wall model; §2.4).

C. Turbopumps

Centrifugal pumps: Euler work, **Wiesner slip**, Cooper-class overall efficiency; hydraulic share is a Gülich **optimal-efficiency** heuristic docked from developed head (not a validated off-design map). NPSH available is station-static diagnostic only. Fixture shaft: bearing/seal Coulomb and viscous loss coefficients as frozen (turbine seal viscous-only).

D. Regenerative cooling

Hot-gas HTC: **Bartz**. Coolant HTC: **Gnielinski + Naraghi** land/fin correction. Liner: 1D radial conduction ODE per section. Coolant is **RP-1**. Film cooling and GG dump into the nozzle are out of scope.

E. Nozzle geometry, field thrust, and startline practice

Divergent wall: parametric **Rao** 80% bell ($\varepsilon = 16$, $R_t = 0.129\,\mathrm{m}$, throat arc factor 0.382 on this freeze). At analysis stop, a volumetric MOC solve uses MCC stagnation (p_0, t_0, γ, r_s) and yields exit-plane integrals plus per-plane mass history. This field coupling is one-way and sequential: the MOC solve consumes the transient model's chamber state at stop and does not feed back into the system solve.

Startline (classical practice; methods hygiene). Sharp Rao throats cannot be seeded with a flat uniform sonic disc at the geometric throat. The live producer uses a mass-conserving curved transonic startline in the Sauer / Kliegel–Levine lineage (right-running characteristic; NASA CR-61332 / NTRS 20030067852 hybrid practice). Standard practice for finite throat curvature. Residual disposition thresholds for the extract are defined below.

Native field-thrust assembly (definitions used throughout):

Disposition (verification): $|r_{\text{conservation}}| \leq 5\%$ pass; 5–15% warn; >15% methods-demo only. Raw r_{network} is a **model-basis** comparison (disclosed separately). Separation: **Schmucker** wall-lip flag only.

We use **verification** for consistency thresholds and regression pins. Comparison to Merlin public numbers is **class-band comparison**, not experimental **validation**.

TABLE I
FIELD-THRUST ASSEMBLY AND MASS-RESIDUAL DEFINITIONS.

Quantity	Definition
Unreconciled field thrust	$F_{\text{field}} = f_{\text{vac}} - p_a A_e - f_{\text{bl}_\text{d}\text{rag}}$ ($k = 1$) — **headline**
Density-linear mass map (diagnostic)	$F' = F_{\text{field}} + (k-1)(f_{\text{mom}} - f_{\text{bl}_\text{d}\text{rag}})$, $k = \dot{m}_{\text{MCC}}/\dot{m}_{\text{field}}$ — co-reported with F_{field} (§4.1); **not** independent validation
Engine Isp (body default)	$\text{Isp}_{\text{eng}} = F/(g_0\,\dot{m}_{\text{prop}})$, $\dot{m}_{\text{prop}} = \dot{m}_{\text{MCC}} + \dot{m}_{\text{GG}}$ (open-cycle total gas-source propellant)
Nozzle-flow Isp (reference)	$\text{Isp}_{\text{noz}} = F/(g_0\,\dot{m}_{\text{field}})$ — component metric on field exit $\dot{m}$; omits GG bleed
Raw field–network delta	$r_{\text{network}} = (\dot{m}_{\text{field}} - \dot{m}_{\text{MCC}})/\dot{m}_{\text{MCC}}$
Marcher conservation residual	$r_{\text{conservation}} = (\dot{m}_{\text{exit}} - \dot{m}_{\text{first}})/\dot{m}_{\text{first}}$

TABLE II
CODE-VERIFICATION ANCHORS AND THEIR ROLES.

Anchor	Role
Vulcain 1 published operating numbers [25]–[30]	Pump ΔP, TC/injector inlet P, packing, TC geometry — component checks (§2.6.1)
SSME / RS-25 throat [23]	HTC **plausibility** (not Merlin cooling validation)
Merlin public disclosures / secondary compilations	Class bands that **guided** case authoring

F. Code-verification anchors on literature engines (supporting)

1) Vulcain 1 component-verification anchors: **Component verification:** the pump, feed-pressure, cooling-channel packing, and thrust-chamber geometry models are checked against **Vulcain 1** literature constants (Kirner [25], Pizzarelli [26][27], Torres [28], EN-AVT-150 [29], SEP/Snecma TC document [30], Brossel/Eury lineage), compiled for traceability in the companion design specification [22] — the same constant surface the automated LOX-pump and TC geometry tests use. The integrated multiphysics case study and MOC-field results are for a **Merlin 1D–class** reconstruction. Vulcain and Merlin share **software methods**, not cycle identity (LOX/LH_2 dual turbopump vs LOX/RP-1 single shaft).

Evidence type is **plausibility / unit-physics**: these anchors exercise the component solvers on a documented LOX/LH_2 engine; the LOX/RP-1 case study stands on its own residuals (§4). LOX pump ΔP is the automated band check; LH pump is characterization only. Cooling packing is geometry/flow bookkeeping, without any wall-T claim. Gas-path R_s/γ "model-sim" rows and Vulcain-2 nozzle-dump notes are omitted as literature anchors.

G. Prior art and methodological distinction

Transient system frameworks. Transient network simulation of liquid rocket engines is a mature field. ROCETS (Pratt & Whitney / NASA MSFC) established the modular pattern — lumped components with quasi-steady maps closed by

TABLE III
VULCAIN 1 COMPONENT-VERIFICATION ANCHORS (TRANSCRIBED FROM THE COMPANION DESIGN-SPECIFICATION COMPILATION [22]; KINDS: SUPPORTED / INFERRED). SOURCE COLUMN CITES THIS PAPER'S REFERENCE LIST ([25]–[30], PLUS [10] FOR TANK-INLET PRESSURE); THE PARENTHESISED Vn TAGS CROSS-REFERENCE THE COMPILATION'S OWN SOURCE NUMBERING FOR TRACEABILITY AGAINST [22].

Quantity	Value	Kind	Source	Automated check
LOX pump ΔP (T16)	$122.8 - 3.5 =$ $\mathbf{119.3}$ bar (TC LOX inlet - tank inlet)	Supported	[29] - [10] (V8-V1)	LOX pump ΔP within published band
Coolant $\dot{m}$ (T16b)	**33.42 kg/s**	Supported	[26] (V7)	Packing + coolant $\dot{m}$ bookkeeping
Cooling channels n (T16b)	**360**	Supported	[25]/[27] lineage (V6/V10)	Same
Throat channel X/Y, land, wall t (T16b)	**1.3 / 11 / 1.0 / 1.0 mm** class	Supported	[27] (V10)	Same
Channel AR band (T16b)	**4.6–8.46**	Supported	[28] (V11)	Same
TC / injector inlet P LH / LOX (T16c)	**141.7 / 122.8 bar**	Supported	[29] (V8)	Constants + pump-band construction
LH TC outlet drop (T16c)	**28 bar** below LH inlet	**Inferred**	derivation note in [22]	Disclosed derivation only
Throat radius R^* (T24v)	**0.127 m**	Supported	[25] (V6)	TC Vulcain geometry / design-point
Nozzle ε base / extension (T24v)	**32 / 45.1**	Supported	[30] (V5)	Same
Axial stations x conv / throat / exp (T24v)	**0.10 / 0.42 / 0.695 m** class	Supported	[25] (V6)	Same

ODE integration — and was applied to the full RL10A-3-3A expander-cycle engine [33]. The European line runs through EcosimPro: the ESPSS libraries add feed, combustion, and turbomachinery components [31] and have been used for full-engine start-up transients [32], alongside the earlier EcosimPro LRE demonstration cited for feed-line heritage [10]. CARINS (CNES/ONERA) targets the same engine-transient prediction problem with an open architecture [35]; NPSS is the U.S. modular propulsion-simulation framework of the same architectural class (air-breathing focus) [34]. Steady algebraic cycle analysis [20][21] and integrated design tools such as RPA [36] complement these with power-balance and quasi-1-D performance at a design point. Throughout this class, nozzle thrust enters through quasi-one-dimensional relations — c^*, C_F, or tabulated performance decks — so the nozzle is a component map inside the network, and no independent field solution exists that could disagree with the network.

Multidimensional nozzle performance. The nozzle-analysis line runs standalone: TDK couples a transonic start-line to an axisymmetric MOC march [6], and the NASA 2D/3D MOC tools document curved-startline practice [7]; JANNAF-style performance prediction sits in the same tradition. These codes take chamber stagnation conditions as *inputs* — prescribed by the user or by a steady cycle balance — and report nozzle performance. A transient system model is outside their scope, and agreement between the field's integrated mass flow and the mass flow of whatever supplied the chamber conditions is not among their reported quantities. Merlin-class reconstructions such as Sippel & Wilken [3] use steady cycle modelling for class studies; subsystem CFD is out of scope here.

Distinction. The two classes report complementary but disjoint quantities: transient frameworks report engine-state histories with map-based nozzle thrust; nozzle codes report multidimensional performance at prescribed chamber conditions. This paper reports the composition of the two on one frozen case — an axisymmetric MOC field evaluated at the chamber stagnation state of an independently solved transient open-cycle network — together with the quantity that only exists once both are present: the system↔field mass-flow residual, graded separately from marcher conservation (r_{network} vs $r_{\text{conservation}}$, §2.5) rather than absorbed into a discharge coefficient or a combustion-efficiency factor. The contribution is therefore the composition and its consistency-gating methodology — frozen inputs, headless extract, separately graded residuals — not feature parity with the frameworks above.

III. CASE DEFINITION AND PARAMETER PROVENANCE

A. Frozen case

All quantitative tables in this paper refer to one frozen Merlin-class open-cycle GG case. Archive identity (for the Zenodo deposit) is recorded once here; the rest of the manuscript refers to it as the **frozen case**.

Regression (**verification** pins, not public validation): end-sample MCC / GG gas $\dot{m}$ at 2.0 s (MCC **296.479**, GG **8.44525** kg/s, $\pm 2\%$ — pinned on the pre-retune freeze; this freeze's end samples, 296.82 / 8.43 kg/s, sit inside the bands). MCC end-sample is a **phase sample** on a bounded oscillation (window mean 296.0, range ~293.9–296.8 kg/s).

Figure 1. Detail of the frozen Merlin-class case in the **Meco Rocket Simulator** layout editor (Loren Aerospace; illustration only): liquid feed and injector branches, single-shaft turbopump with starter, the GG → turbine hot-gas path, and the MCC chamber–throat–nozzle chain with regenerative-cooling joints and wall solids — the layer-2 baseline element

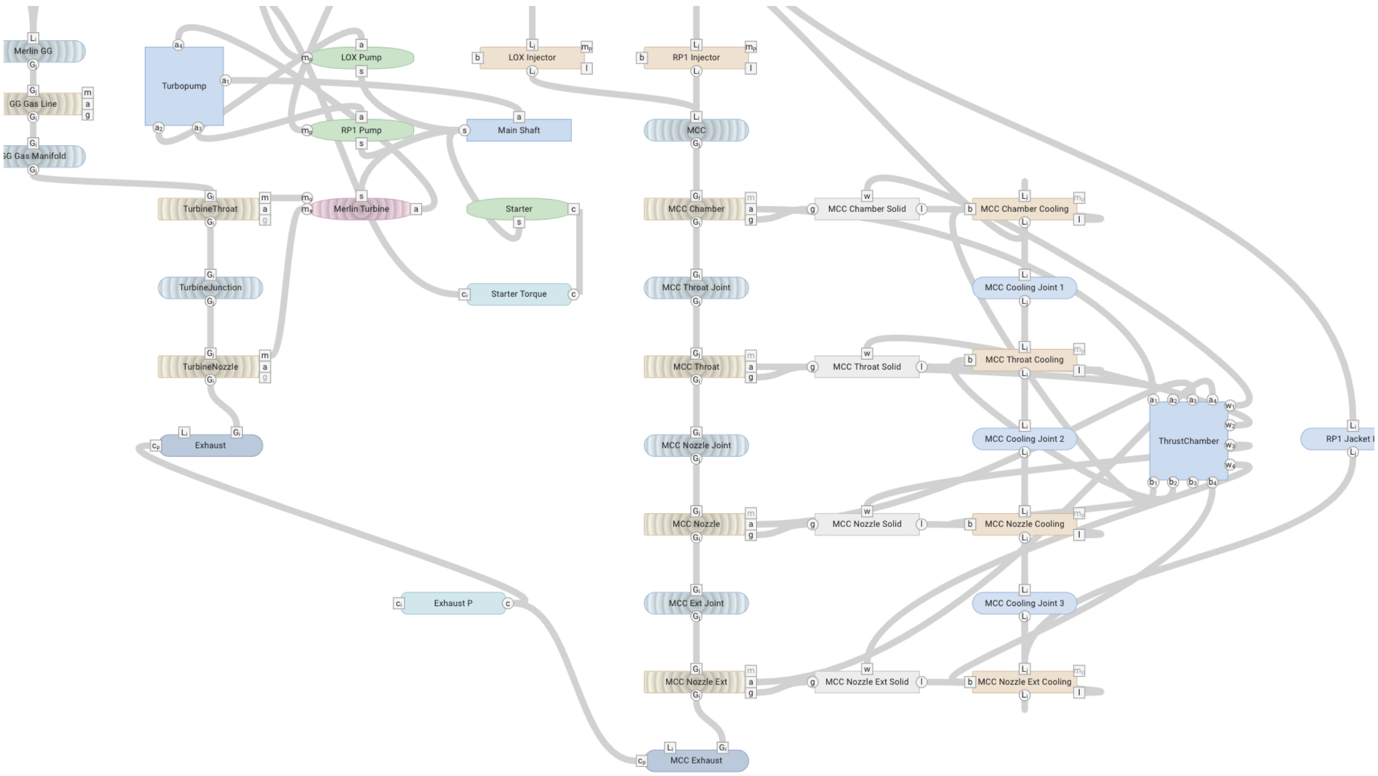

Fig. 1. Merlin-class case in the Meco layout editor

TABLE IV
FROZEN-CASE IDENTITY AND ARCHIVE PINS.

Item	Value
Case	Merlin full-engine open-cycle GG fixture
Input deck checksum (md5)	`64f364d6a43c50d7a2f7f77b ddef235f`
Software archive id	`00312a51` (retuned-freeze snapshot; v0.5 deposit was `b11a0aec`)
Horizon	2.0 s
Injectors	LOX/RP-1 discharge-law orifices (baseline element class)
Extract tables	Settle windows + MOC field thrust (headless)

classes of §3.2 as authored. Quantitative values in this paper derive from the headless LorenLib extract on the frozen fixture, not from product UI readouts.

1) Data availability (short): At first public preprint DOI (**engrXiv** + **Zenodo**), readers should obtain:

1. This PDF
2. Extract tables and case definition (checksum above)
3. Companion **design specification** with attribution, licence, and reproducibility notes (run recipe for the shipped headless executable if regenerating tables — not required to *read* this paper)

B. What was fixed vs what emerged

Public Merlin data underdetermine a unique numerical fixture. Agreement with Merlin-class headline numbers is **uninterpretable** unless the reader can see which quantities were inputs, which knobs were set by the author, and which outputs genuinely emerged. We separate four layers so the reader can distinguish model definition from parameter selection, and class-band proximity from calibration.

1. **Literature / method-fixed** — correlations and contour families used as-is: slip, HTC maps, Rao construction, property tables, separation criterion form.
2. **Baseline system definition** — *which* element types and couplings the case uses (capability of the system model). Choosing orifice injectors instead of plain pipe branches is **model definition**, not parameter tuning.
3. **Author-selected parameters** — continuous (and discrete level) values inside that baseline that a human set for the frozen case (geometry, C_d, loss coefficients, schedule levels). These are **not** claimed unique from public data. They were, however, selected at physically plausible Merlin-class scales — feedline bores and lengths, manifold/dome volumes, and injector geometry triangulated from operating-point mass flows, an assumed Δp band, and LMDE pintle heritage (worked provenance ships as a note in the archive's freeze data) — so emergent band agreement is not the product of unphysical compensating values. The chamber contraction ($\varepsilon_c = 3.5$) and chamber-to-pintle proportion ($D_c/D_p = 3.0$) follow pintle-engine design guidance: pintle chambers run longer and at higher contraction ratio than conventional engines to support the

TABLE V
LITERATURE / METHOD-FIXED CORRELATIONS (LAYER 1).

Item	Notes
Wiesner slip; Cooper overall η; Gülich optimal-efficiency hydraulic share	Fixed method maps
Bartz / Gnielinski / Naraghi HTC	Correlation-level
Rao 80% bell construction; throat-arc factor 0.382 (Huzel–Huang class)	Contour family
O–F / fluid property tables	Offline generators
Schmucker separation flag form	Criterion only

TABLE VI
BASELINE SYSTEM DEFINITION (LAYER 2) — ELEMENT CLASSES.

Choice	Role in the baseline
LOX / RP-1 injectors as **discharge-law orifices**	Correct element class for injector ΔP–$\dot{m}$ (vs plain friction ducts)
Shaft bearing/seal loss fittings as first-class torque sinks	Mechanical loss model present (vs lossless shaft)
Feedline K-loss fittings	Component pressure-loss (K-factor) models in the liquid path — unlined flex-bellows, tee-elbow, and ball-valve entries on the freeze
Single-shaft turbopump + GG + MCC regen chain	Cycle topology for an open-cycle GG
Chained control-parameter startup graph	Transient schedule architecture
Post-stop MOC on Rao wall + native field-thrust assembly	Nozzle evaluation path for this paper

injector's recirculation zones [38].

4. **Emergent** — solve outputs on that frozen case (pressures, ω, field $\dot{m}$, F_{field}, residuals, wall T). **Regression pins** (end-sample gas $\dot{m}$ $\pm 2\%$) fix settle reporting for this case only — verification, not public validation. **Class-band comparison** situates emergent numbers against public/inferred Merlin bands without treating proximity as calibration.

Sensitivity note. Varying *author-selected* parameters (layer 3) can move settle $\dot{m}$ and shaft power by **O(10%)**. Tabulated numbers in this draft always refer to the frozen case in §3.1; other parameter choices are not claimed unique.

Concrete instances of each layer for this case follow.

Literature / method-fixed (layer 1). Correlations and maps taken as-is:

Baseline system definition (layer 2). Element classes that define *what physics the baseline can express*:

Author-selected parameters (layer 3; this frozen case). Values as shipped in the frozen JSON (illustrative; full file is authoritative):

TABLE VII
AUTHOR-SELECTED PARAMETERS ON THE FROZEN CASE (LAYER 3; ILLUSTRATIVE).

Parameter	Freeze value (examples)	Effect
LOX orifice	$C_d = 0.7$, $r = 4.8\,\text{mm}$ (∅9.6 mm), $n = 72$, $L \approx 14\,\text{mm}$	LOX feed ΔP / $\dot{m}$ share
RP-1 orifice	$C_d = 0.8$, annulus radii 84.2/80.45 mm, $n = 1$, $L = 50\,\text{mm}$	Fuel feed ΔP / $\dot{m}$ share
GG turbine stage geometry	e.g. tip radius $0.109\,\text{m}$, rotor height $0.016\,\text{m}$, rotor/stator counts and admission as frozen	GG $\dot{m}$, torque, power
LOX GG feed bore	~$2.9\,\text{mm}$ class	GG O/F and bleed
Shaft loss coefficients	Coulomb + viscous coefficients on the five bearing/seal fittings (turbine seal viscous-only)	Settled ω, torque residual
GG schedule level / clamp	engaged GG ramp targets 0.75 (LOX) / 0.76 (RP-1) on freeze	Engaged GG operating point
TC design geometry	$R_t = 0.129\,\text{m}$, chamber $r = 0.241\,\text{m}$ ($\varepsilon_c = 3.5$), $\varepsilon = 16$, length fraction 0.8	Chamber/nozzle scale (model choice)
Pump design-point geometry	$\beta_2, r_1, r_2, b_2, \ldots$	Pump ΔP at speed
Integration horizon	2.0 s	Horizon for quasi-steady tables

TABLE VIII
PUBLIC MERLIN 1D HARDWARE VS FIXTURE REALIZATION (DISCLOSED IDEALIZATIONS).

Aspect	Public Merlin 1D	Frozen fixture
Spin start	Helium turbine spin start	Applied shaft starter torque (20 N·m), scheduled off early in the startup sequence, before the valve ramps
Ignition	TEA–TEB pyrophoric ignition	Instantaneous equilibrium at combustion heads (§2.2)
Injector	Pintle injector	Lumped discharge-law orifice set — radial holes + annulus (§2.2)

Hardware idealizations (disclosed). Three places where the fixture deliberately stands in for public Merlin 1D hardware practice (hardware kinds per the provenance ledger [24]):

Figure 2. Pintle-injector configuration realised by the frozen fixture's lumped orifice parameters (schematic; not a Merlin drawing; all dimensions are radii). (a) Meridional half-section: RP-1 annular sheet (radii 84.2/80.45 mm, $C_d = 0.8$) along the pintle post (r 80.45 mm) inside the chamber (r 241.3 mm; contraction ratio $\varepsilon_c = 3.5$, $D_c/D_p = 3.0$); LOX injected radially at the tip. (b) Developed tip circumference: LMDE-heritage staggered rows — 3 rows of 24 circular holes ($n = 72$, $r = 4.8\,\text{mm}$, $C_d = 0.7$), rows offset 7.2 mm (a 2.4 mm overlap, 50% of the hole radius), minimum inter-row land 3.2 mm. The chamber proportions follow pintle-engine design guidance — longer, higher-contraction chambers supporting the injector's recirculation zones [38]. Worked provenance

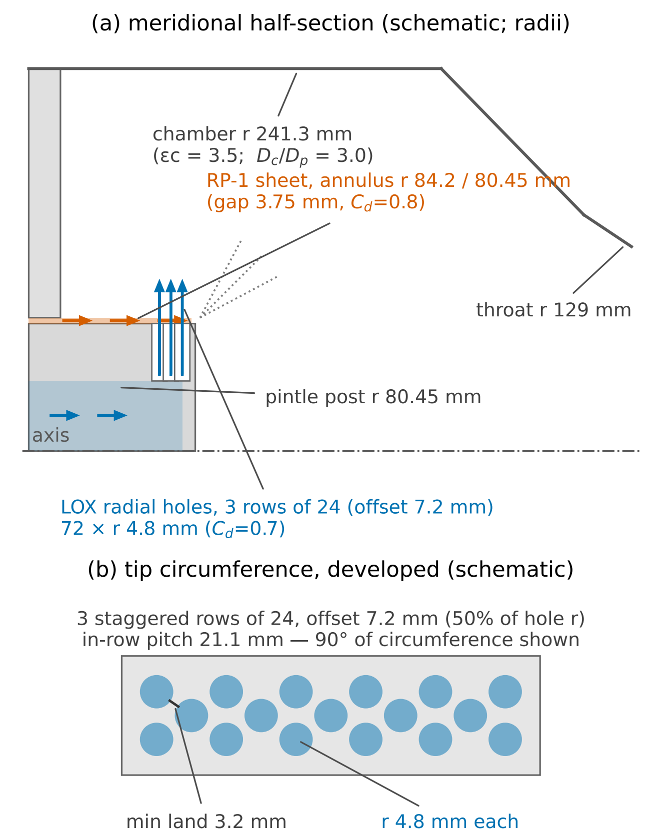

Fig. 2. Pintle-injector configuration schematic

TABLE IX
EMERGENT OUTPUTS ON THE FROZEN CASE (LAYER 4).

Quantity	Notes
MCC / GG gas $\dot{m}$ @ 2.0 s	Emergent; regression-pinned ±2%
ω, node P, pump ΔP, wall T	Emergent; class-band **comparison** only
Field $\dot{m}$, F_{field}, conservation residual, network delta	Emergent MOC + live stagnation
F'	Derived diagnostic (k-map); co-reported with F_{field} in §4.1

ships as a note in the archive's freeze data.

Not claimed: a multi-objective fit to Merlin flight F/Isp/$\dot{m}$. **Claimed:** gas $\dot{m}$ regression pins (±2%) lock the **emergent** settle after the fixture is frozen — verification, not public validation.

Emergent on this frozen case (layer 4). Solve outputs (and derived diagnostics) on the lock above:

IV. RESULTS

A. Field thrust, mass residuals, and Isp on the freeze

On the freeze producer (classical mass-conserving curved startline; §2.5), the extract reports:

Chamber state at extract: $p_0 \approx 10.14\,\mathrm{MPa}$, $t_0 \approx 3671\,\mathrm{K}$, $\gamma \approx 1.215$, $r_s \approx 369\,\mathrm{J/(kg\cdot K)}$. Paper MOC resolution: 48 streamlines from the wall, 8 radial intervals, max axial step $0.015R_t$. Pass/warn thresholds are methods bookkeeping (§2.5).

TABLE X
MASS DIAGNOSTICS ON THE FREEZE PRODUCER (HEADLESS EXTRACT).

Diagnostic	Value
$\dot{m}_{\mathrm{sim}}$ (network MCC)	296.82 kg/s
1-D isentropic choke at $a^* = \pi R_t^2$	296.82 kg/s (matches network on this freeze)
$\dot{m}_{\mathrm{first}}$ (curved start plane)	~288.9 kg/s
$\dot{m}_{\mathrm{field}}$ (exit)	291.53 kg/s
$r_{\mathrm{conservation}} = (\dot{m}_{\mathrm{exit}} - \dot{m}_{\mathrm{first}})/\dot{m}_{\mathrm{first}}$	**+0.92% (pass)**
$r_{\mathrm{network}} = (\dot{m}_{\mathrm{field}} - \dot{m}_{\mathrm{sim}})/\dot{m}_{\mathrm{sim}}$	**-1.78%**
$f_{\mathrm{bl_d rag}}/f_{\mathrm{vac}}$	0.63%

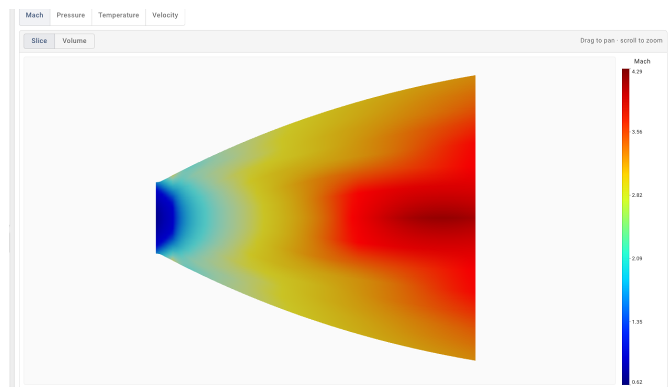

Fig. 3. Meridional Mach slice of the MOC field

Figure 3. Meridional Mach-number slice of the axisymmetric MOC field on the frozen case (Rao wall, $\varepsilon = 16$), rendered interactively in **Meco Rocket Simulator** (illustration only). The rendering visualises the same post-stop field summarised here; quantitative values (thrust, $\dot{m}$, residuals) come from the headless extract tables, not from this view.

Reading the two residuals. $r_{\mathrm{conservation}}$ grades the marcher (first curved plane → exit) on a fixed wall/mesh. r_{network} compares that exit field $\dot{m}$ to the **independently solved** network MCC $\dot{m}$ — a **model-basis** cross-check, not a second copy of the same integral. The **~-1.8%** network delta on this freeze is therefore a research quantity in its own right. Closing it by re-authoring geometry or startline to force exact agreement would **obscure** the system↔field interface this paper is built to expose. A mesh / startline / throat-curvature convergence study that tests whether the delta asymptotes is a natural follow-on; explaining a stable finite basis difference is preferred to forcing $r_{\mathrm{network}} = 0$.

Negative control (optional note). A constant-z Sauer seed on this wall produced ~13–14% field mass deficit vs 1-D choke (residual **warn**); mesh refinement did not close it; restoring the classical curved startline brings the conservation residual back inside the **pass** band ($\leq 5\%$, §2.5: +0.92% on the freeze). It is retained as an internal regression check that the residual disposition responds.

Field thrust on the freeze — **both mass bases in one table.** Headline is unreconciled F_{field} ($k = 1$). Density-linear F' uses

TABLE XI
FIELD THRUST AND ENGINE ISP AT BOTH MASS BASES (UNRECONCILED FIELD VS DENSITY-LINEAR MCC MAP; SAME FREEZE).

Ambient	p_a (Pa)	$F_{\rm field}$ (kN)	$\rm Isp_{eng}$ (s)	F' (kN)	$\rm Isp'_{eng}$ (s)	Schmucker
SL	101325	**831.2**	**277.7**	846.8	282.9	unflagged
near-vac	100	**915.8**	**305.9**	931.5	311.2	unflagged

the same MOC integrals with $k = \dot{m}_{\rm MCC}/\dot{m}_{\rm field} = 1.018$ ($\dot{m}_{\rm field} = 291.53$, $\dot{m}_{\rm MCC} = 296.82$ kg/s) so the $\sim 1.8\%$ field–network mass residual is **visible as a thrust lever** rather than absorbed into a single reconciled number. Formula detail: §2.5 and Appendix B.

Isp denominators (open-cycle):

- **Engine Isp** (paper default on either F): $\text{Isp} = F/(g_0\,\dot{m}_{\rm prop})$, $\dot{m}_{\rm prop} = \dot{m}_{\rm MCC} + \dot{m}_{\rm GG}$ (end-sample **305.25 kg/s**). Counts GG exhaust as spent propellant.
- **Nozzle-flow Isp** (component reference): $\text{Isp}_{\rm noz} = F/(g_0\,\dot{m}_{\rm field})$ — omits GG bleed; overstates open-cycle engine Isp by $\sim 4.7\%$ on this freeze when F is held fixed.

How to read the table. Bold columns are the **headline** (unreconciled field + engine Isp on total propellant). F' / $\rm Isp'_{eng}$ are the density-linear map of the **same** field to network MCC $\dot{m}$ — a disclosed approximation rather than a re-solved nozzle. By construction (Appendix B), the single mass-basis factor $k = \dot{m}_{\rm MCC}/\dot{m}_{\rm field} = 1.018$ drives the **entire** 15.6 kN sea-level separation between $F_{\rm field}$ and F' (and the 5.2 s engine-Isp separation): $F' - F_{\rm field} = (k-1)(f_{\rm mom} - f_{\rm bl_drag})$, with no other physics differing between the two columns. Near-vac is **not** Merlin Vacuum (ε=16 booster wall). Class-band comparison of Isp must use **engine** Isp (either column), not nozzle-flow Isp.

B. Case study: quasi-steady operating point of the frozen reconstruction

We avoid calling the last window "steady." **Quasi-steady settled window:** last 0.1 s mean $\bar{x}$ and σ_x; report end-sample separately when the window contains a bounded oscillation (MCC $\dot{m}$ does). The oscillation's origin (feed–chamber hydraulic coupling vs integration effects) has not been isolated on this freeze; it is bounded at $\sigma/\text{mean} \approx 0.44\%$, and both window statistics and the end-sample are reported so it is visible rather than averaged away.

Values below are **emergent on the frozen fixture**, compared to public/inferred bands that **guided case authoring**—not experimental validation. Band entries are compiled from public sources — the Falcon User's Guide [1], manufacturer remarks [2], Sippel & Wilken [3], and manufacturer interview statements — with the per-number source and kind ledger (Public / Supported / Inferred / Secondary) in the companion design specification [24].

C. Wall temperatures (uncalibrated system outputs)

Cooling claim restraint. Throat hot wall sits inside the ~800–900 K Estimate band. Coolant-side throat wall **numerically overlaps** literature ranges sometimes associated with hydrocarbon thermal degradation. That overlap is **qualitative plausibility only**. With **one-way** coolant coupling, **no** coolant bulk-enthalpy ODE, and **no** coking/film physics, these temperatures **cannot** support a coking-propensity or cooling-design prediction claim. They are uncalibrated system outputs, reported for methods completeness. A coolant bulk-enthalpy ODE plus a calibrated wall model is the future-work path to a defensible coking-propensity assessment.

D. Coupled-system bookkeeping (engine level)

Nozzle-side $r_{\rm conservation} = +0.92\%$ (§4.1) sets the reporting standard; the **engine system** receives the same explicit treatment below.

Liquid $\leftrightarrow$ gas mass (end-sample / last window).

Full **species** continuity through regen is **not** claimed (thermodynamic head tables, not species-closed liquid↔gas; §2.2, §6). The ~0.2% liquid–gas mass delta is bookkeeping at extract resolution, not a first-law or atom balance.

Shaft torque / power closure (window means).

Residual is consistent with shaft-loss fittings and residual inertia on the settled window.

Energy. No full-engine first-law closure (one-way regen; table coolant T).

E. Transient dynamics

Window means (0.1 s centres) from the settle extract on the frozen case. Shaded bands are window min–max. These traces are **main-paper evidence**: the model integrates **time-dependent ODEs** (liquid capacitance–inertance, gas-network state, shaft inertia) under a chained control-parameter schedule. A steady algebraic cycle sheet cannot produce Figures 4–5. They are a dynamics demonstration for this model class, not a reconstruction of the Merlin flight start sequence.

Figure 4. (a) $P_{\rm MCC}(t)$, $P_{\rm GG}(t)$ (MPa) and (b) shaft $\omega(t)$ (rad/s); lines are 0.1 s window means, shaded bands window min–max. Fuel-lead schedule: GG and MCC pressures and shaft speed rise together through ~ 0.5–1.2 s (coupled feed–shaft–gas response), then settle toward the $t = 2.0$ s analysis stop used for §4.1–§4.4 tables. The settle window is quasi-steady with a small MCC $\dot{m}$ oscillation (§4.2).

Figure 5. LOX feed, RP-1 feed, and MCC gas $\dot{m}$ (kg/s); lines are 0.1 s window means, shaded bands window min–max. Liquid feeds lead; chamber gas $\dot{m}$ tracks the schedule into the ~305 kg/s end-sample bookkeeping of §4.4. The multi-physics spin-up is the observable that distinguishes this formulation from a single power-balance settle card.

TABLE XII
QUASI-STEADY FREEZE WINDOW VS PUBLIC/CLASS BANDS (CASE OUTCOMES).

Quantity	Freeze (last 0.1 s unless noted)	Public / class band	Comment
MCC $\dot{m}$ (window)	296.0 ± 1.3 kg/s	—	End-sample pin 296.82; σ/mean $\approx$ 0.44%
GG $\dot{m}$	8.430 ± 0.004 kg/s	no Public $\dot{m}_{gg}$	Quiet
Total gas $\dot{m}$ (end)	**305.3 kg/s**	~305 kg/s (Inferred)	On freeze, inside band used in authoring
GG bleed	**2.76%**	~4–8.6% power-balance envelope	**Below** envelope — report
Shaft ω	3955 ± 0.17 rad/s (~37.8 krpm)	~36 krpm Public	+~5% on freeze
Turbine power $\tau\omega$	~6.43 MW	~7.46 MW Public oral	-14% on freeze
MCC P (window)	10.09 ± 0.03 MPa	9.7 MPa Public	+~4% on freeze
MCC combustion t_0 (window)	3669.0 ± 2.6 K	~3650 K Estimate	+~0.5%; end-sample 3670.6 K equals the §4.1 MOC chamber state
GG P	8.45 MPa	~7–11 MPa Supported	Inside broad band
GG combustion t_0 (turbine inlet)	1130.4 ± 0.6 K	~1000–1100 K Estimate	Slightly above heritage band — report
LOX / RP-1 feed $\dot{m}$	208.9 / 95.6 kg/s	~214 / ~91 Inferred	
Overall O/F (feeds)	~2.19	~2.35 Inferred	Fuel-rich of band
LOX / RP-1 pump ΔP	13.7 / **20.2** MPa	cycle-budget / 15–20 MPa class	RP-1 top of band; **not** 200 atm calibration
LOX NPSH_A	0.63 m	—	Thin margin

TABLE XIII
SECTION WALL TEMPERATURES ON THE FREEZE (UNCALIBRATED OUTPUTS OF THE ONE-WAY WALL MODEL; REPORTED FOR COMPLETENESS, NOT DESIGN PREDICTION).

Section	Hot-gas wall T (K)	Coolant-side wall T (K)
Throat	813	623
Chamber	700	631
Nozzle	619	574
Extension	461	447

TABLE XIV
ENGINE-LEVEL LIQUID–GAS MASS CLOSURE (END-SAMPLE / LAST WINDOW).

Closure	Freeze	Normalized residual
MCC gas + GG gas (end)	296.82 + 8.43 = **305.25** kg/s	— (definition of total gas $\dot{m}$)
LOX + RP-1 feed (window mean)	208.9 + 95.6 $\approx$ **304.5** kg/s	$(\dot{m}_{\text{liq}} - \dot{m}_{\text{gas}})/\dot{m}_{\text{gas}} \approx \mathbf{-0.25}\%$
MCC pin phase vs window mean	end 296.82 vs window 296.0 ± 1.3	oscillation scale σ/mean $\approx$ 0.44%; residual within that band

TABLE XV
SHAFT TORQUE AND POWER CLOSURE (WINDOW MEANS).

Quantity	Value	Normalized residual
τ_{turb}	$1625.1\,\text{N}\cdot\text{m}$	—
$\tau_{\text{LOX}} + \tau_{\text{RP1}}$	$-861.2 - 762.2 = -1623.3\,\text{N}\cdot\text{m}$	—
Torque residual $\tau_{\text{turb}} + \tau_{\text{LOX}} + \tau_{\text{RP1}}$	$\approx +1.75\,\text{N}\cdot\text{m}$	$\sim \mathbf{0.11}\%$ of $\lvert\tau_{\text{turb}}\rvert$
Turbine power $\tau\omega$	$\approx 6.43\,\text{MW}$	—
Pump mechanical load	$\approx 6.42\,\text{MW}$	power mismatch $\sim \mathbf{0.11}\%$ of turbine power

V. DISCUSSION

Principal contribution. The principal contribution is the coupled architecture and its consistency methodology; the Merlin-class reconstruction serves as a representative numerical case. The centre is the **coupled open-cycle system itself**: liquid capacitance–inertance feeds, LMA gas network, shaft dynamics, regen walls, equilibrium thermochemistry, orifice injectors, and a post-stop MOC field on a shared chamber state—with frozen inputs and a headless extract that regenerates the tables. That composition (and the claim discipline

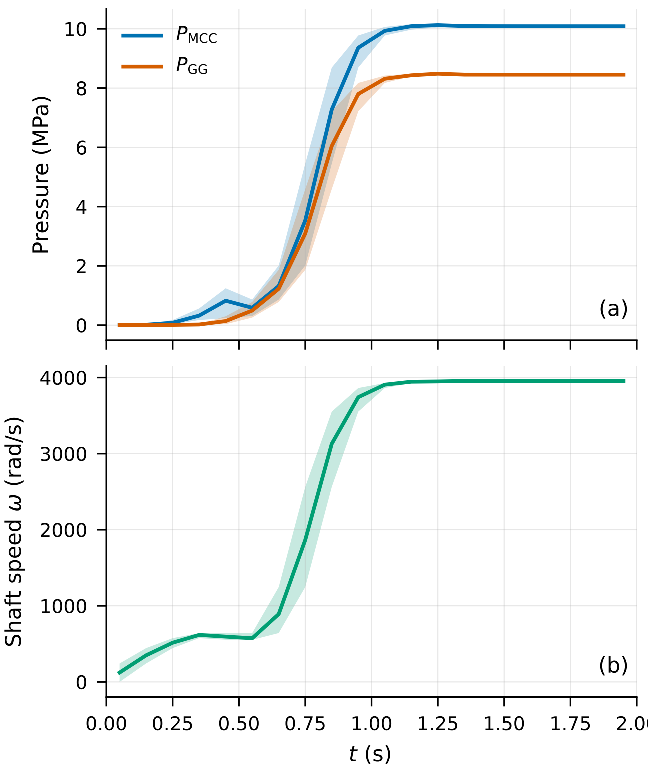

Fig. 4. Chamber and GG pressure and shaft speed vs time

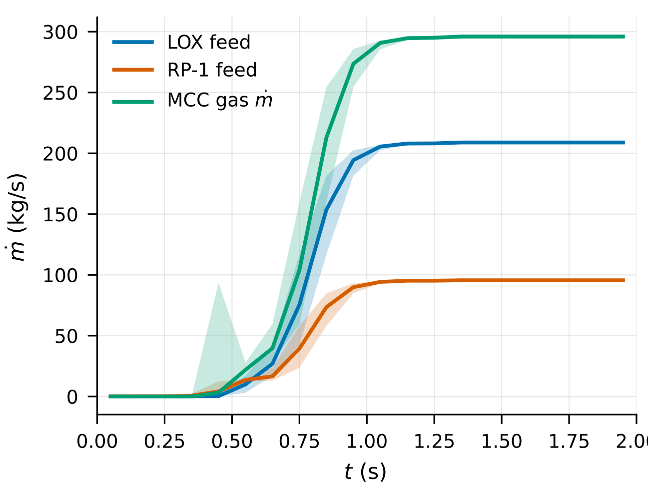

Fig. 5. Feed and chamber mass flow vs time

around it) is the contribution; classical curved-startline practice and density-linear F' bookkeeping are **supporting infrastructure** (§2.5, §4.1, Appendix B).

Mass gates; r_{network} as research quantity. Automated $r_{\text{conservation}}$ / r_{network} reports keep the stack honest at the system↔field interface. Marcher conservation is verification hygiene; the disclosed ~1–2% network delta is a **cross-model residual to study** (§4.1). A constant-z seed is retained as a **control** in §4.1 that the gates fire.

Case study in context. On the **frozen** fixture, total gas $\dot{m}$ is near the ~305 kg/s inferred band and $F_{\text{field}} \approx 830\,\text{kN}$ is near the public 845 kN class; the §3.2 hierarchy (method-fixed / baseline / author-selected / emergent / class-band comparison) is what keeps that proximity legible as a case outcome rather than as calibration success. Selected continuous parameters (orifice C_d, shaft loss coeffs, GG level, R_t, ...) are underdetermined by public data; O(10%) sensitivity under parameter changes is expected. That is distinct from defining the baseline element set (e.g. orifice injectors vs plain branches).

System conservation at the same standard as the nozzle. Liquid–gas mass and shaft torque/power residuals are reported with normalized percentages in §4.4 (~0.2% mass, ~0.1% torque), parallel to the nozzle +0.92% conservation row.

Bleed, power, and Isp. Low GG bleed tracks turbine power below the ~7.5 MW Public oral class while pumps run high discharge, with GG turbine-inlet $t_0 \approx 1130\,\text{K}$ just above the ~1000–1100 K heritage estimate — reported as case outcomes. Engine Isp must use MCC+GG propellant; nozzle-only Isp flatters open-cycle performance.

Cooling / combustion. Uncalibrated one-way walls: temperature overlap with hydrocarbon degradation ranges is **qualitative plausibility only** (§4.3). Equilibrium tables only—no kinetics or spray fidelity (SSME/Vulcain anchors are component code verification; §2.6).

VI. Limitations

- Fixed-step RK4; stiffness knobs affect transients.
- One-way regen; no boiling/coking/film; no GG dump into nozzle. Wall T overlap with degradation ranges is **qualitative only** (§4.3).
- Axisymmetric meridional MOC only.
- **Combustion / injectors:** instantaneous equilibrium table lookup only—**no** finite-rate chemical kinetics, ignition delay, droplet atomization/breakup, vaporization time scales, 3D pintle spray patternation, or high-frequency combustion-instability physics, and no η_{c^*} scalar — combustion is ideal equilibrium, an upper c^* bound (§2.2). Injectors are orifice hydraulics (Δp–$\dot{m}$), not multiphase spray combustion.
- Pump η_h share heuristic; NPSH diagnostic.
- No full MVac reconstruction.
- No full first-law engine energy closure; liquid↔gas mass continuity at combustion heads is thermodynamic (tables), not species-closed.
- Public Merlin tags mix Public / Supported / Inferred / Secondary; SL Isp lacks a primary pin in our compilation.
- Continuous fixture parameters are author-selected under class bands, not uniquely fixed by public data (§3.2).

VII. Conclusions

We describe a **coupled open-cycle** liquid-rocket system architecture (liquid capacitance–inertance, LMA gas network, shafts, regen walls, equilibrium thermochemistry tables, orifice injectors) with a post-stop MOC-field thrust pipeline and a headless extract that grades system↔field mass residuals. On a frozen Merlin-class case (baseline system + selected parameters, §3), first-to-exit conservation **passes** (+0.92%) with a disclosed -1.78% field–network delta kept as a **model-basis research quantity**; system liquid–gas and shaft torque/power residuals are reported to the same explicit standard (~0.2% / ~0.1%). Engine Isp on total propellant (~305 kg/s) is ~277.7 s with unreconciled SL F_{field} ~831 kN; the density-linear mass-basis map places the same field at 282.9 s / 846.8 kN, the entire separation carried by the measured $k = 1.018$ (§4.1, Appendix B) — case outcomes, not flight validation. Transient window series (§4.5) show multi-physics spin-up that a steady algebraic cycle cannot produce — at interactive cost (§2.1), supporting rapid human- or optimizer-in-the-loop case iteration. Parameter-sensitivity and throttled operating-point sweeps (e.g. over the GG schedule level), and a Merlin Vacuum–class case ($\varepsilon \approx 165$ nozzle extension vs the $\varepsilon = 16$ booster wall here), are natural follow-on studies at that cost; every tabulated number in this paper remains on the single frozen case (§3.1). The primary value is the **architecture, its composition, and transparent residual reporting**; the Merlin-class reconstruction is a representative case rather than a validated twin.

VIII. Software and data availability

Extract tables, the frozen case definition (checksum §3.1), figures, and the headless executable + data snapshot that regenerates the tables are archived on **Zenodo**. The dynamical model and MOC field are implemented in **LorenLib** (Open Space Launch Ltd); licence and availability terms are in the companion design specification in the Zenodo package. The interactive authoring environment used for case authoring and inspection, **Meco Rocket Simulator** (mecorocketsimulator.com), is a commercial desktop product of Loren Aerospace Ltd that embeds LorenLib; it is optional — reproducing the tabulated results requires only the Zenodo archive (§2.1.1).

Acknowledgments

Implementation of the dynamical model and MOC field is **LorenLib**; case authoring, interactive inspection, and optional figures used **Meco Rocket Simulator** (see *Software and data availability*). Scientific tables in this paper were regenerated with headless LorenLib extracts on the frozen fixture (§2.1.1). The author is affiliated with Open Space Launch Ltd (LorenLib development) and Loren Aerospace Ltd (Meco Rocket Simulator).

IX. Declaration of generative AI and AI-assisted technologies

During the preparation of this work, the author used generative-AI tools (including OpenAI ChatGPT and AI coding assistants) for software-development assistance, literature discovery, analysis support, critical review, and manuscript drafting and editing. Quantitative results were generated by the frozen LorenLib implementation and extraction harness (§3.1); AI outputs were not used as substitutes for simulation data. The author reviewed and verified all AI-assisted material and takes full responsibility for the content of this paper. A record of material tools and major uses is retained by the author.

References

Case engine and class data

1. SpaceX, *Falcon User's Guide*, Space Exploration Technologies Corp. (current public revision as used for Merlin class bands) — pad timeline / hold-down envelope; Merlin-class public F, Isp, ε bands.
2. Mueller, T., remarks at AIAA/ASME/SAE/ASEE Joint Propulsion Conference (2011) — manufacturer comments on Merlin ε / chamber-pressure "sweet spot" (secondary report of oral remarks; not a peer-reviewed paper).
3. Sippel, M. & Wilken, J., "Selection of propulsion characteristics for systematic assessment of future European RLV-options," *CEAS Space Journal*, 17 (2025), doi:10.1007/s12567-024-00564-w — peer-reviewed Merlin-1D-class modelling study used for Supported P_c ceiling / GG pressure-class comparison only (the ~12 MPa P_c and ~11 MPa GG values are the authors' modelling selections, not SpaceX disclosures).

Transonic startline / MOC (prior art applied)

4. Sauer, R., "General characteristics of the flow through nozzles at near critical speeds," NACA TM-1147 (translation of original German work, 1947 lineage) — transonic throat approximation used in TDK-class startline practice.
5. Kliegel, J. R. & Levine, J. N., "Transonic flow in small throat radius of curvature nozzles," *AIAA Journal*, 7(7):1375–1378 (1969) — small throat radius-of-curvature transonic field / discharge-coefficient regime.
6. Nickerson, G. R. et al., *Two-Dimensional Kinetics (TDK) Nozzle Performance Computer Program*, NASA CR-61332 (and updates) — hybrid transonic → MOC startline practice as cited in §4.1.
7. Rice, T. et al., "NASA 2D/3D Method of Characteristics tools," NASA NTRS 20030067852 — curved initial data / Kliegel–Levine–Hall family; constant-z vs characteristic startline discussion.
8. Rao, G. V. R., "Exhaust nozzle contour for optimum thrust," *Jet Propulsion*, 28(6):377–382 (1958); subsequent contoured-bell approximations (1958–61 lineage) — parametric Rao wall used here.
9. Almqvist, M., separation / side-load notes (Luleå University of Technology, 2005) — Schilling/Schmucker separation pressure-ratio forms as used here.

System solvers (liquid capacitance + gas network)

10. Margarit i Bel, N. & Sánchez, M. M., "Simulation of a Liquid Rocket Engine," *1st Meeting of EcosimPro Users*, UNED, Madrid, 3–4 May 2001 — system-level LRE liquid

dynamics / EcosimPro heritage for lumped feed modelling (capacitance–inertance class).

11. MIT OpenCourseWare, 16.512 *Rocket Propulsion* lecture notes — cryogen compressibility / hydraulic capacitance scales for LOX-class κ.
12. Sultanian, B. K., *Gas Turbines: Internal Flow Systems Modeling*, Cambridge University Press, Cambridge Aerospace Series (2018) — 1-D compressible **flow network** modelling (mass coupling, nodal solution) informing the gas-network architecture.
13. Levenberg, K., "A method for the solution of certain non-linear problems in least squares," *Q. Appl. Math.*, 2:164–168 (1944); Marquardt, D. W., "An algorithm for least-squares estimation of nonlinear parameters," *J. Soc. Indust. Appl. Math.*, 11(2):431–441 (1963) — damped least-squares / LMA outer-loop **name** heritage for the residual-minimising gas solve (implementation is problem-specific).
14. Osiadacz, A. J., *Simulation and Analysis of Gas Networks*, Gulf Publishing / E. & F.N. Spon (1987 and related pipeline-network literature) — classical steady/unsteady **gas network** simulation context (complementary to CUP flow-network treatment [12]).

Turbomachinery, cooling, system context

15. Wiesner, F. J., "A review of slip factors for centrifugal impellers," *ASME J. Eng. Power*, 89(4):558–566 (1967) — slip factor.
16. Gülich, J. F., *Centrifugal Pumps*, Springer — hydraulic-efficiency share / optimal-efficiency heuristics.
17. Bartz, D. R., "A simple equation for rapid estimation of rocket nozzle convective heat transfer coefficients," *Jet Propulsion*, 27(1):49–51 (1957) — rocket nozzle convective HTC.
18. Gnielinski, V., "New equations for heat and mass transfer in turbulent pipe and channel flow," *Int. Chem. Eng.*, 16:359–368 (1976) — turbulent duct Nu correlation.
19. Naraghi, M. H. & Foulon, M., "A simple approach for thermal analysis of regenerative cooling of rocket engines," ASME IMECE2008-67988 (2008) — regen land/fin network.
20. Huzel, D. K. & Huang, D. H., *Modern Engineering for Design of Liquid-Propellant Rocket Engines*, AIAA Progress in Astronautics and Aeronautics / NASA SP-125 lineage — system LRE methods context.
21. Sutton, G. P. & Biblarz, O., *Rocket Propulsion Elements*, Wiley — cycle context (quasi-1D F is **not** paper thrust).
22. Vulcain 1 operating-constants compilation — traceability table in the companion design specification [24], aggregating [25]–[30]; component-verification anchors only, not an independent source document.
23. Rocketdyne, *SSME Orientation* (1998) / MCC life-prediction notes / Wang et al. HTC studies — RS-25 throat HTC **plausibility** anchors (not Merlin cooling validation).
24. Companion design specification for this paper (methods contracts, attribution, reproducibility manifest) — **Zenodo package**; not required to read the scientific claims.

Vulcain 1 compiled methods sources (§2.6.1 triangulation table)

25. Kirner, E., et al., "Development Status of the Vulcain Thrust Chamber" (1993) — thrust-chamber geometry (throat radius, injector-plate radius, axial stations) and cooling-channel packing lineage.
26. Pizzarelli, M., et al., "Trade-off analysis of high-aspect-ratio cooling channels for rocket engines" (2013) — coolant mass-flow anchor.
27. Pizzarelli, M., et al., "Evolution of cooling-channel properties for varying aspect ratio" (2016) — throat cooling-channel dimensions; packing lineage.
28. Torres, Y., et al., "Heat and mass transfers in curved cooling channels of rocket engines" (2020) — cooling-channel aspect-ratio band.
29. Haidn, O. J., "Advanced Rocket Engines," NATO RTO-EN-AVT-150, paper 6 (2008) — Vulcain 1 thrust-chamber / injector inlet pressures.
30. *Vulcain Rocket Engine — Thrust Chamber*, technical document (SEP/Snecma lineage; archived with the companion compilation [22]) — nozzle expansion ratios (base 32 / extension 45.1).

Transient system frameworks and integrated performance tools (§2.7)

31. Moral, J., Pérez Vara, R., Steelant, J. & De Rosa, M., "ESPSS Simulation Platform," *Space Propulsion Conference*, San Sebastián, 3–6 May 2010 — European Space Propulsion System Simulation libraries on EcosimPro (feed, combustion, turbomachinery components).
32. Di Matteo, F., De Rosa, M. & Onofri, M., "Start-Up Transient Simulation of a Liquid Rocket Engine," AIAA 2011-6032, 47th AIAA/ASME/SAE/ASEE Joint Propulsion Conference (2011), doi:10.2514/6.2011-6032 — full-engine start-up transient on ESPSS-class components.
33. Binder, M., "An RL10A-3-3A Rocket Engine Model Using the Rocket Engine Transient Simulator (ROCETS) Software," AIAA 93-2357 (1993), doi:10.2514/6.1993-2357 — modular transient network framework applied to a full expander-cycle engine.
34. Lytle, J. K., "The Numerical Propulsion System Simulation: An Overview," NASA/TM-2000-209915 (2000) — modular multidisciplinary propulsion-simulation framework (air-breathing focus).
35. Ordonneau, G., Albano, G. & Masse, J., "CARINS: A Future Versatile and Flexible Tool for Engine Transient Prediction," *4th International Conference on Launcher Technology "Space Launcher Liquid Propulsion"*, Liège, 3–6 December 2002 — CNES/ONERA open engine-transient simulation tool.
36. Ponomarenko, A., "RPA: Design Tool for Liquid Rocket Engine Analysis" (2010) — integrated equilibrium thermochemistry and quasi-1-D nozzle performance at a prescribed operating point.

Injector orifice hydraulics (§2.2)

37. NASA SP-8089, *Liquid Rocket Engine Injectors*, NASA Space Vehicle Design Criteria (Chemical Propulsion), March 1976 (NTRS 19760023196) — measured orifice discharge-coefficient classes (figs. 13, 15) and as-drilled vs lapped fabrication-scatter caveat.
38. Dressler, G. A. & Bauer, J. M., "TRW Pintle Engine Heritage and Performance Characteristics," AIAA 2000-3871 (2000), doi:10.2514/6.2000-3871 — pintle-engine design fundamentals and LMDE heritage; pintle chambers run longer and at higher contraction ratio than conventional engines to support the injector's recirculation zones (p. 6 and Table 1).

Appendix A — Extract tables (pointer)

Settle-window and MOC thrust tables ship with this manuscript and with the **Zenodo** archive. Regeneration commands, archive pins, licence, package checklist, **preprint changelog**, and the editorial **claim audit (T11)** live in the companion design specification (Zenodo package) — this body assumes no repository access and does not carry process history.

Appendix B — Density-linear mass map (formula detail)

Numbers for F' and $\mathrm{Isp}'_{\mathrm{eng}}$ are in the §4.1 results table (same rows as F_{field}). This appendix records the **map** so the body table is fully specified.

$$F' = F_{\mathrm{field}} + (k-1)(f_{\mathrm{mom}} - f_{\mathrm{bl_drag}}), \quad k = \dot{m}_{\mathrm{MCC}}/\dot{m}_{\mathrm{field}}.$$

On this freeze $k = 1.018$ ($\dot{m}_{\mathrm{MCC}} = 296.82$, $\dot{m}_{\mathrm{field}} = 291.53$ kg/s). The map is the closed form for scaling exit-plane density by k on a **frozen** MOC shape (momentum and shear scale; pressure integral and $-p_a A_e$ do not). It is a first-order diagnostic in $(k-1)$: it does not capture the boundary-layer, wall-pressure, or shock-structure shifts that a re-marched field at matched $\dot{m}$ would show, and it is not a substitute for re-solving the field. $\mathrm{Isp}'_{\mathrm{eng}} = F'/(g_0\,\dot{m}_{\mathrm{prop}})$ with $\dot{m}_{\mathrm{prop}} = 305.25\,\mathrm{kg/s}$ (MCC+GG). Proximity of $\mathrm{Isp}'_{\mathrm{eng}}$ SL to the public ~282 s band is a freeze outcome under that map. Product UI cards use the same native assembly.